



AKADEMIA GÓRNICZO-HUTNICZA IM. STANISŁAWA STASZICA W KRAKOWIE
WYDZIAŁ FIZYKI I INFORMATYKI STOSOWANEJ

KATEDRA ODDZIAŁYWAŃ I DETEKCJI CZASTEK

Praca dyplomowa

First application of the diffusion and transformer models for medical
CT scans analysis in scope of MonAI platform

Pierwsze zastosowanie modeli dyfuzyjnych i modeli typu
transformer do analizy medycznych skanów tomografii
komputerowej w ramach platformy MonAI

Autor:	Piotr Harmuszkiewicz
Kierunek studiów:	Informatyka Stosowana
Opiekun pracy:	prof. dr hab. inż. Tomasz Szumlak

Kraków, 2023

Acknowledgement

I would like to express gratitude to Zuzanna Harmuszkiewicz for providing me with valuable advice and insight on the topic of my thesis and for taking time to read and review my work.

Contents

1	Goals and motivation of the thesis.	5
2	Theoretical Basis	6
2.1	Convolutional neural networks	6
2.2	Generative models	7
2.3	Diffusion models	7
2.3.1	Forward diffusion process	7
2.3.2	Reparameterization trick	7
2.3.3	Reverse diffusion process	8
2.3.4	Position embedding	9
2.4	Attention	9
2.4.1	Attention block	9
3	Implementation of the model	11
3.1	Project environment	11
3.1.1	Python	11
3.1.2	PyTorch	11
3.1.3	Monai	11
3.1.4	Huggingface diffusers	12
3.1.5	Hardware	12
3.2	Implementation	12
3.2.1	Resnet	12
3.2.2	Attention block	14
3.2.3	Downsample and Upsample	15
3.2.4	Resnet downsample and upsample	15
3.2.5	Attention downsample and upsample	16
3.2.6	Mid block	17
3.2.7	Network architecture	18
3.2.8	Training parameters	19
3.2.9	Training script	20
3.3	Dataset	20
4	Results	22
4.1	Loss	22
4.2	Generated CT scans	24
4.2.1	Examples	24
4.2.2	Visual Realism and Quality	27

4.2.3	Variability and Diversity	27
4.2.4	Comparison to original data	27
4.3	Limitations	27
4.4	Future Directions	27
Bibliographic		27

Chapter 1

Goals and motivation of the thesis.

This master thesis aimed to prepare a diffusion model able to generate new medical CT scans and perform quality analysis of obtained results. The motivation for the implementation of the project was solving the problem of insufficient amount of training data, required for different machine learning solutions used in medical field. The first chapter is an introduction to the study, explaining the goal and motivation of the project. Next chapter contains theoretical foundations, the chapter covers essential concepts like diffusion models and attention. In the third chapter the implementation of the project was explained, detailing the project environment, model architecture, training process and dataset. The final chapter presents the outcomes, which are analyzed in terms of – visual quality, diversity, and are compared to original data. This chapter also presents limitations and conclusion.

Chapter 2

Theoretical Basis

2.1 Convolutional neural networks

A convolutional neural network (CCN) is a type of deep neural model that is suited for grid-like data (e.g. images, which are two dimensional grid of pixels). CNNs use a mathematical operation called convolution that combines two functions to produce third function. In machine learning we usually use kernel, which is a small matrix. The kernel is moved in horizontal and vertical direction over the input data and applying kernel results in matrix, which is called feature map. The values of kernels are trainable neural network's parameters. [17] [23]

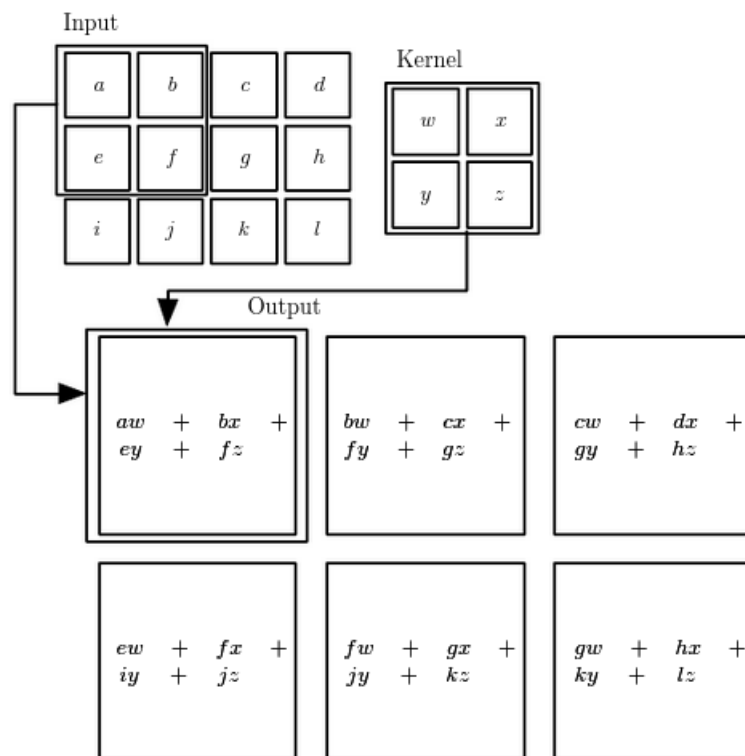


Figure 2.1: Example of kernel and 2D convolution [17]

2.2 Generative models

Generative models are type of algorithms that aim at creating new examples similar to data from dataset. Generative models learn probability distribution of training dataset and are able to generate complicated data based on this distribution.

2.3 Diffusion models

Diffusion models are type of generative models, that aim at modelling distribution of data from a given dataset. They use Markov chain, which represent sequence of steps in which small random noise is added to data and then model learns to gradually reverse diffusion steps. Diffusion model contains two components: forward diffusion process and reverse diffusion process.

2.3.1 Forward diffusion process

During forward diffusion process we define Markov chain with T steps, which are more and more distorted samples from dataset. The result is a sequence: x_1, \dots, x_T of samples with distribution $q(x_t|x_{t-1})$:

$$q(x_t|x_{t-1}) = N(x_t; \sqrt{1 - \beta_t}x_{t-1}, \beta_t I)$$

$$q(x_{1:T}|x_0) = \prod_{t=1}^T q(x_t|x_{t-1})$$

In each step we add a small amount of Gaussian noise with the variance β_t multiplied by an identity matrix (due to multi-dimensional data) and the mean value: $\sqrt{1 - \beta_t}x_{t-1}$. For $T \rightarrow \infty$, x_T is an isotropic Gaussian distribution, however for well-chosen values of T and β_1, \dots, β_T it is nearly an isotropic Gaussian distribution and is sufficient for diffusion models.

β_t is constant increased with step t according to a variance schedule, linear function can be used e.g. $B_1 = 10^{-4}$, $B_T = 0.02$ for $T = 1000$. [1]

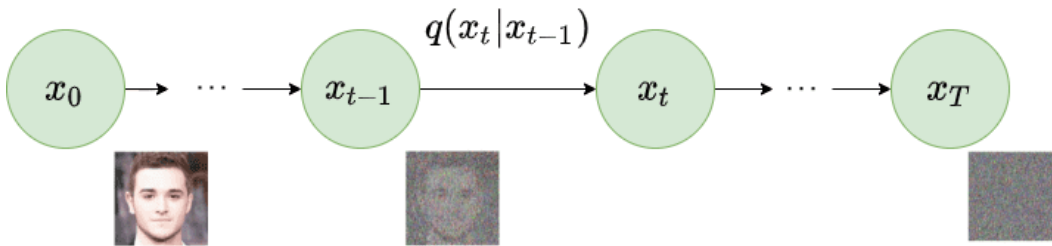


Figure 2.2: Example of Markov chain for an image [1]

2.3.2 Reparameterization trick

The basic idea of the reparameterization trick is to express a random variable sampled from a certain distribution as a deterministic function of a separate random variable and a

fixed parameter. This reparameterization allows for the separation of the randomness in the model from the gradient computations, which makes the optimization process more stable. Instead of directly sampling from the distribution (usually a Gaussian), we sample from a standard Gaussian distribution (mean=0, variance=1) and then transform this sample using the learned mean and variance parameters. Mathematically, we can denote the random variable as z and its distribution as $q(z|x)$, the trick involves representing z as:

$$z = \mu + \sigma \odot \epsilon,$$

where:

- μ - mean value learned by network
- σ - standard deviation learned by network
- ϵ - sample from Gaussian distribution ($\epsilon \sim N(0, I)$)
- \odot - element-wise multiplication

Now we can rewrite formula for $q(x_t|x_{t-1})$ using reparameterization trick as:

$$q(x_t|x_{t-1}) = \sqrt{1 - \beta_t}x_{t-1} + \sqrt{\beta_t}\epsilon$$

Let $\alpha_t = 1 - \beta_t$, $\bar{\alpha}_t = \prod_{i=1}^t \alpha_i$, so:

$$\begin{aligned} q(x_t|x_{t-1}) &= \sqrt{\alpha_t}x_{t-1} + \sqrt{1 - \alpha_t}\epsilon \\ q(x_t|x_{t-2}) &= \sqrt{\alpha_t\alpha_{t-1}}x_{t-2} + \sqrt{1 - \alpha_t\alpha_{t-1}}\epsilon \\ q(x_t|x_0) &= \sqrt{\bar{\alpha}_t}x_0 + \sqrt{1 - \bar{\alpha}_t}\epsilon \end{aligned} \tag{2.1}$$

To get n th element from Markov chain we do not need to apply Gaussian noise n times, which is slow for bigger values of n . It is enough to use an equation 2.1. [6]

2.3.3 Reverse diffusion process

The idea behind reverse diffusion process is to undo the forward process and remove noise that was added. The reverse process is also a Markov chain but this time neural network calculates the next element. Let p_θ be a reverse process function, which is probability density function.

$$p_\theta(x_{0:T}) = p(x_T) \prod_{t=1}^T p_\theta(x_{t-1}|x_t)$$

$$p_\theta(x_{t-1}|x_t) = N(x_{t-1}; \mu_\theta(x_t, t), \Sigma_\theta(x_t, t))$$

In our case, variance is known: $\Sigma_\theta(x_t, t) = \beta_t I$, so the model needs to predict only the mean: $\mu_\theta(x_t, t)$.

To train the network loss function is required, which is defined as negative log-likelihood: $-\log(p_\theta(x_0))$. However it is not easily computable, because $p_\theta(x_0)$ depends on the whole Markov chain. The solution is to use variational lower bound of the function:

$$-\log(p_\theta(x_0)) \leq -\log(p_\theta(x_0)) + D_{KL}(q(x_{1:T}|x_0)||p_\theta(x_{1:T}|x_0))$$

D_{KL} is Kullback–Leibler divergence which measures the distance between two probability distributions. [11] The equation can be simplified [2] and it will result in loss function: $L = ||\epsilon - \epsilon_{\theta}(x_t, t)||^2$, which is just mean square error of applied noise and predicted noise. [8]

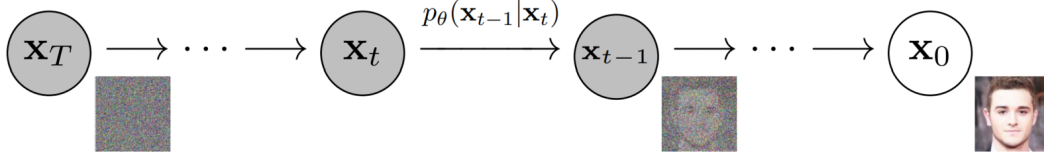


Figure 2.3: Example of reverse diffusion process for image [1]

2.3.4 Position embedding

Given that the neural network shares parameters across the entire Markov chain, we have the option to provide the model with additional information regarding its position within the Markov chain. This can be achieved in two ways: either by introducing a separate argument or by adopting a method similar to how transformers handle it, which involves using position embedding. Position embedding operates by assigning a unique vector representation to each step in the sequence, based on sine and cosine functions. This results in distinct embeddings for various positions. When these positional embeddings are integrated into the input data, the model gains the capability to simultaneously consider both the content of the elements and their positions in the sequence. This enhancement significantly improves the model's ability to effectively comprehend and process data and to be aware of the specific noise level it is currently processing. [18] [19]

2.4 Attention

Attention, in the context of machine learning and natural language processing, is a mechanism that allows models to focus on specific parts of input data while making predictions or generating output. The concept of attention draws inspiration from human cognitive processes, where we naturally pay varying degrees of attention to different parts of information when processing it. Attention mechanisms are particularly useful in tasks where the model needs to consider different parts of input data with varying levels of importance or relevance. [22]

2.4.1 Attention block

To use this mechanism we need to implement an attention block. An attention block is a component in neural network architectures that implements an attention mechanism. It is one of the building blocks used in diffusion model. The attention block typically takes in a set of input representations and computes attention weights to emphasize the importance of different elements within the input. These elements could be words in a sentence, pixels in an image, or any other kind of structured data. The attention weights

are then used to compute a weighted sum of the input representations, resulting in an enriched representation that captures contextual information and relationships between elements.

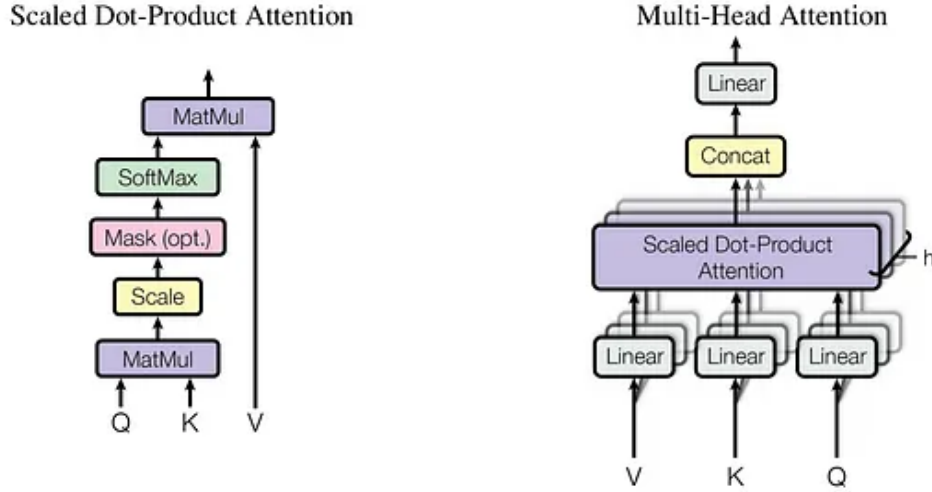


Figure 2.4: Mutli-Head Attention block [19]

Scaled dot-product attention can be describe with:

$$Attention(Q, K, V) = softmax(\frac{QK^T}{\sqrt{d_k}})V$$

Input of multi-headed attetion block is:

- query - represents the element that we are interested in understanding
- key - holds information used to assess the importance of other elements
- value - contains the actual content we want to focus on

All of these values are the same at the beginning.

In essence, the attention mechanism computes scores by comparing the query with keys. These scores reflect how much attention each element deserves. Then, these scores are used to blend the values together, forming an output representation that captures the essence of the input sequence. [19] [20] [21]

Chapter 3

Implementation of the model

This chapter presents the details of the project implementation: description of the development environment and the tools used during development. It will also describe dataset, implementation of the model and some details of selected aspects of the project.

3.1 Project environment

During development the following tools were used:

- Python
- PyTorch
- Monai
- Hugging Face diffusers

3.1.1 Python

Python is a high-level, and widely used programming language known for its simplicity, readability, and extensive libraries. In the context of machine learning, Python is popular due to its rich ecosystem of libraries, frameworks, and tools that make it easier to implement and experiment with various machine learning algorithms and techniques. [24]

3.1.2 PyTorch

PyTorch is an open-source machine learning framework that is used for developing and training machine learning models. PyTorch's central concept is the tensor, a multi-dimensional array, which is used for numerical computations and supports GPU acceleration for faster processing. The framework includes multiple tools to make it straightforward to design and build neural networks and has user-friendly API. [25]

3.1.3 Monai

MONAI (Medical Open Network for AI) is an open-source framework built on PyTorch, designed exclusively for deep learning in medical imaging. It simplifies tasks like data

handling, model creation, training, and deployment for medical image analysis. MONAI focuses on challenges unique to this domain, making it easier to develop and deploy AI models for tasks connected with healthcare. [26]

3.1.4 Huggingface diffusers

Diffusers is an open-source library based on PyTorch. It offers framework for building U-Net models and a lot of functionality used during training like noise scheduler. It also offers pre-trained networks and much more. The library is modular, which allows creating custom models and training pipelines. The library is easy to use and has good documentation. [27]

3.1.5 Hardware

Throughout the project, Nvidia Titan RTX GPU was used, equipped with 24GB of memory for the training and testing of networks. This GPU is compatible with CUDA, a platform that allows general-purpose computing on the GPU, and it is integrated into Pytorch.

3.2 Implementation

The source code is available at the link below:

<https://github.com/Harmek59/diffusion-ct>

Implementation of the model was base on the implementation of: UNet2DModel from diffusers library. The model was adapted to work with 3 dimensional data. The model consists of few building blocks:

- Resnet
- Attention
- Downsample block
- Upsample block
- Midblock

3.2.1 Resnet

ResNet (Residual Network) is a type of neural network design for very deep architectures. It uses residual blocks that let the network learn and improve the difference between input and output. This makes training deep networks easier and helps avoid vanishing gradient problems. [29] Resnet block are the main building blocks of the network. They were proven to provide good results in image processing and are especially useful in deep networks.

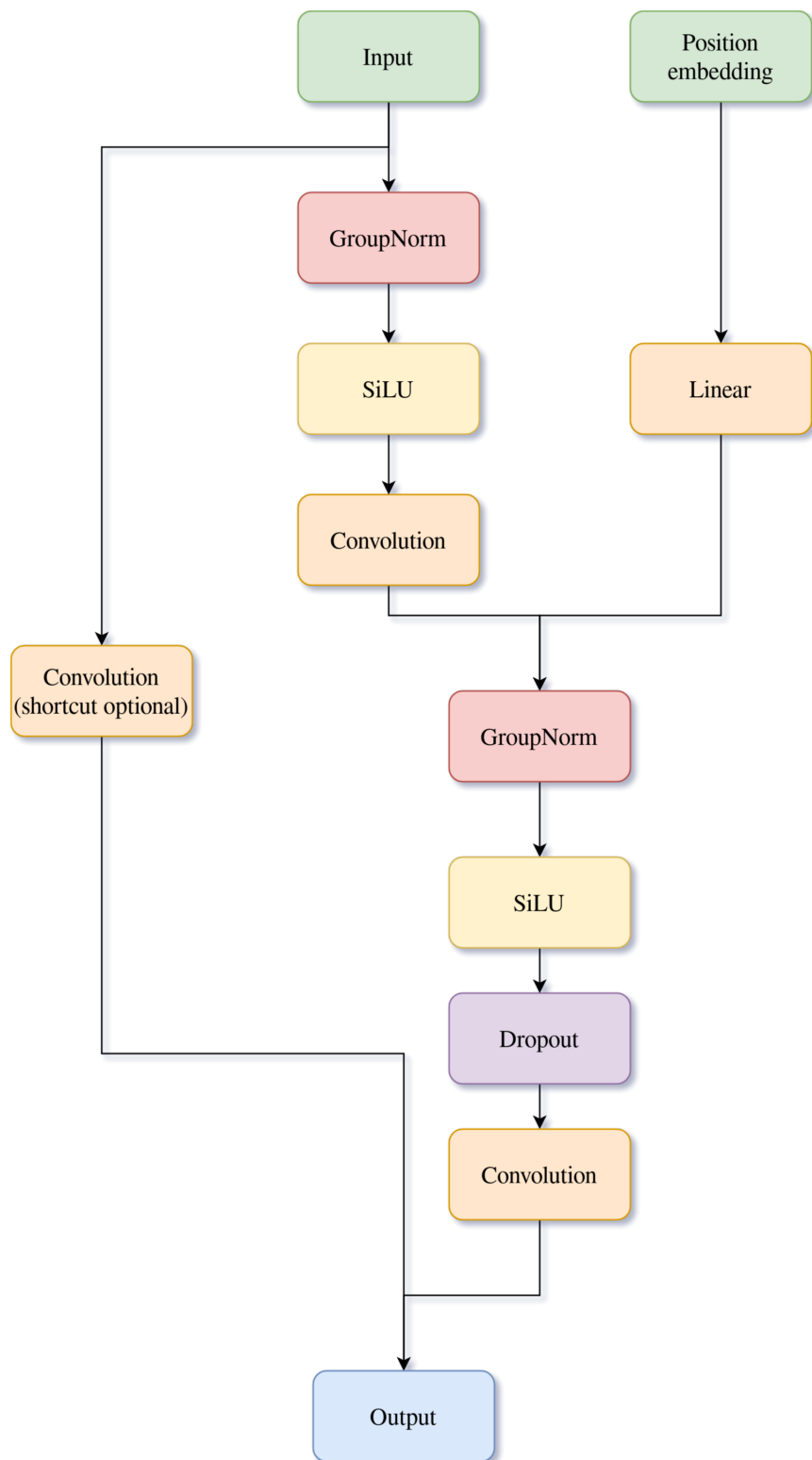


Figure 3.1: Resnet block architecture diagram

3.2.2 Attention block

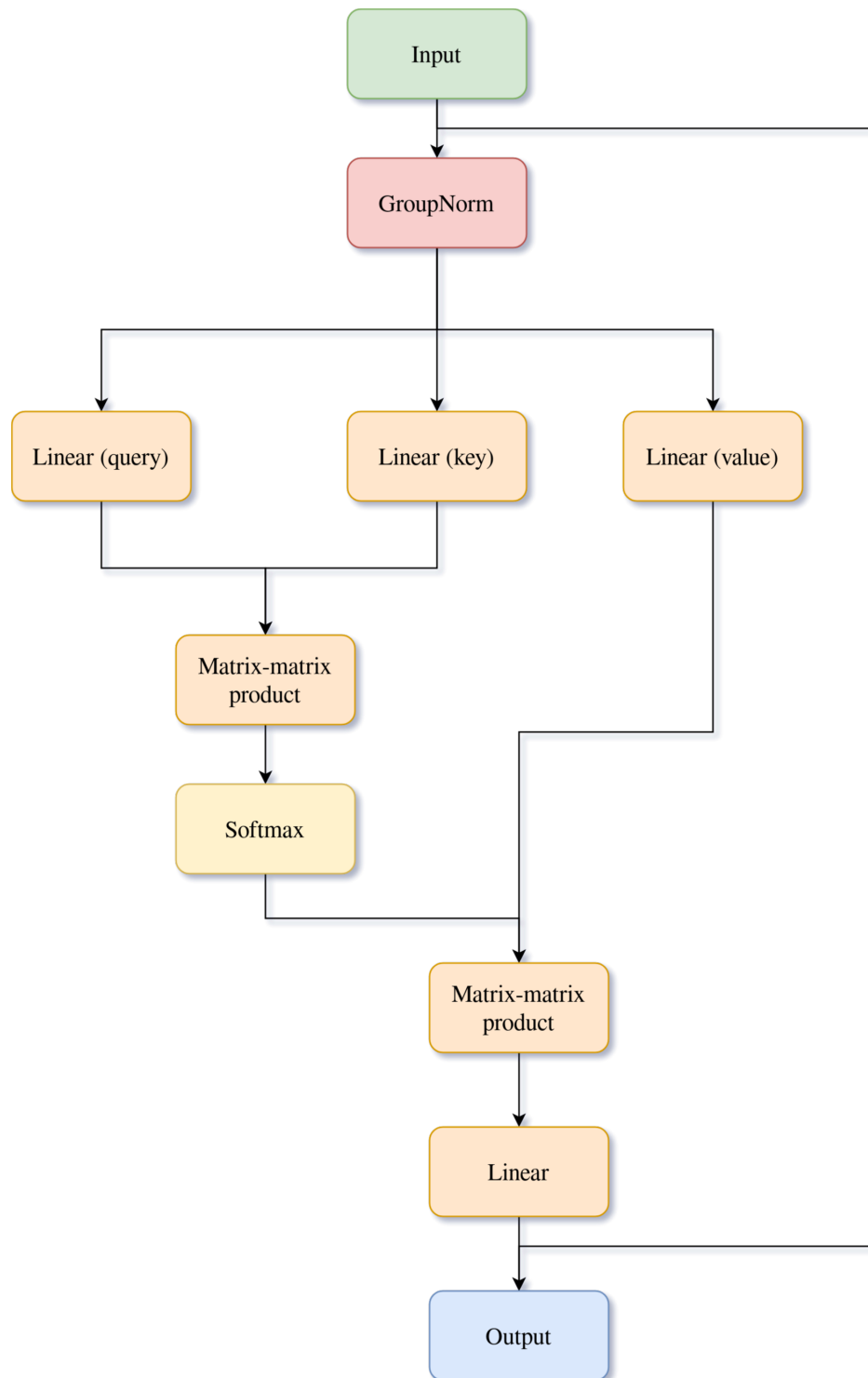


Figure 3.2: Attention block architecture diagram

3.2.3 Downsample and Upsample

Downsample and upsample blocks are simple blocks that reduce or recover dimensions of input data and adjust number of channels. Using them we can obtain certain size of latent space.

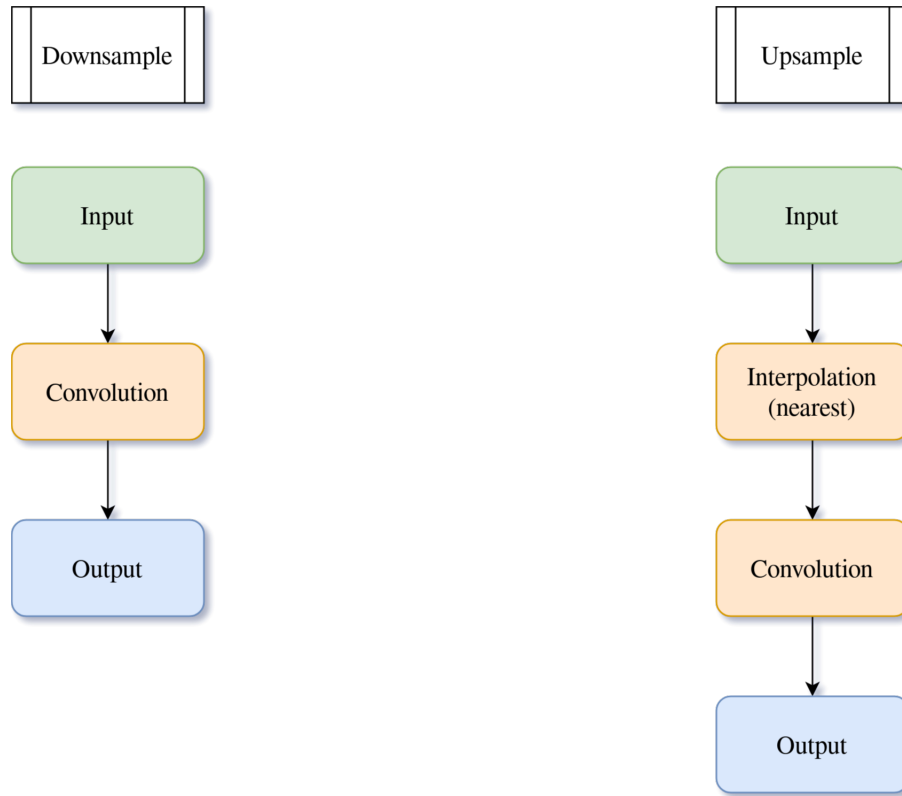


Figure 3.3: Downsample and upsample block architecture diagram

The modules above were used to build the more complex ones which are presented below. The modules below have two inputs or outputs depending on whether they are up or down. The output from the down blocks are directly connected with the input from up blocks.

3.2.4 Resnet downsample and upsample

These modules use resnet blocks and downsample or upsample blocks.

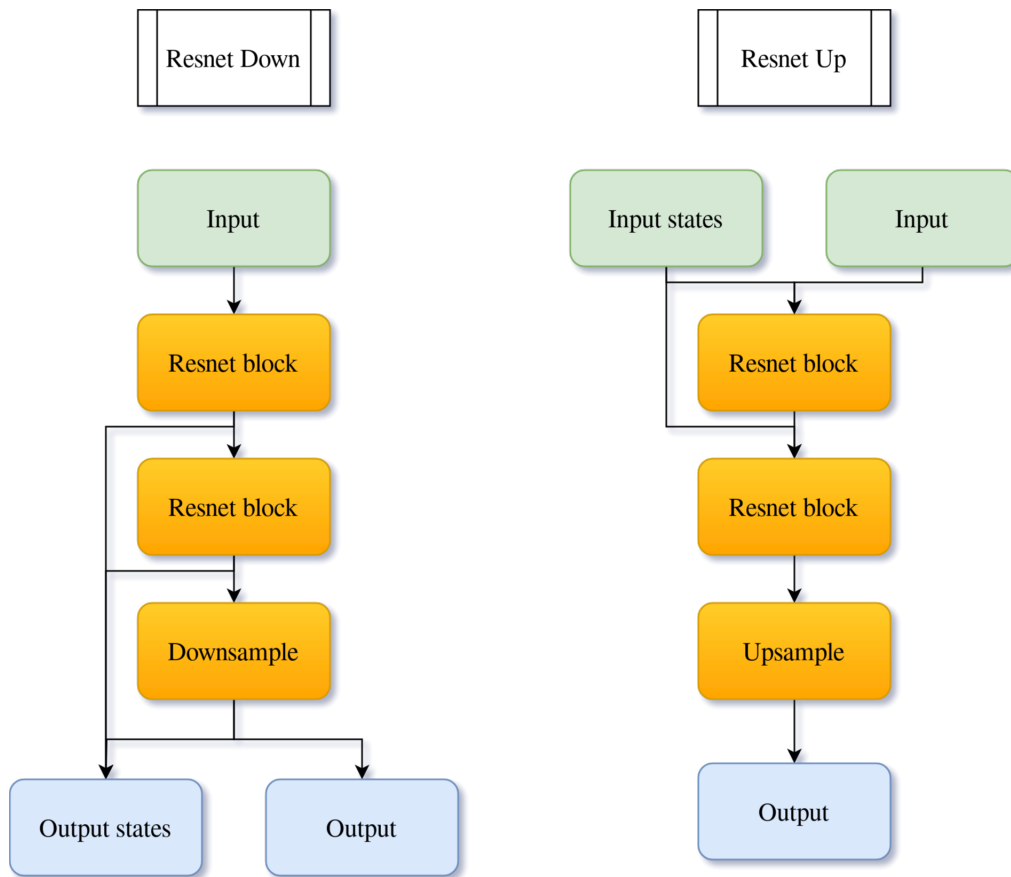


Figure 3.4: Restnet downsample and upsample block architecture diagram

3.2.5 Attention downsample and upsample

These modules are similar to downsample and upsample but have additional attention blocks after every resnet block.

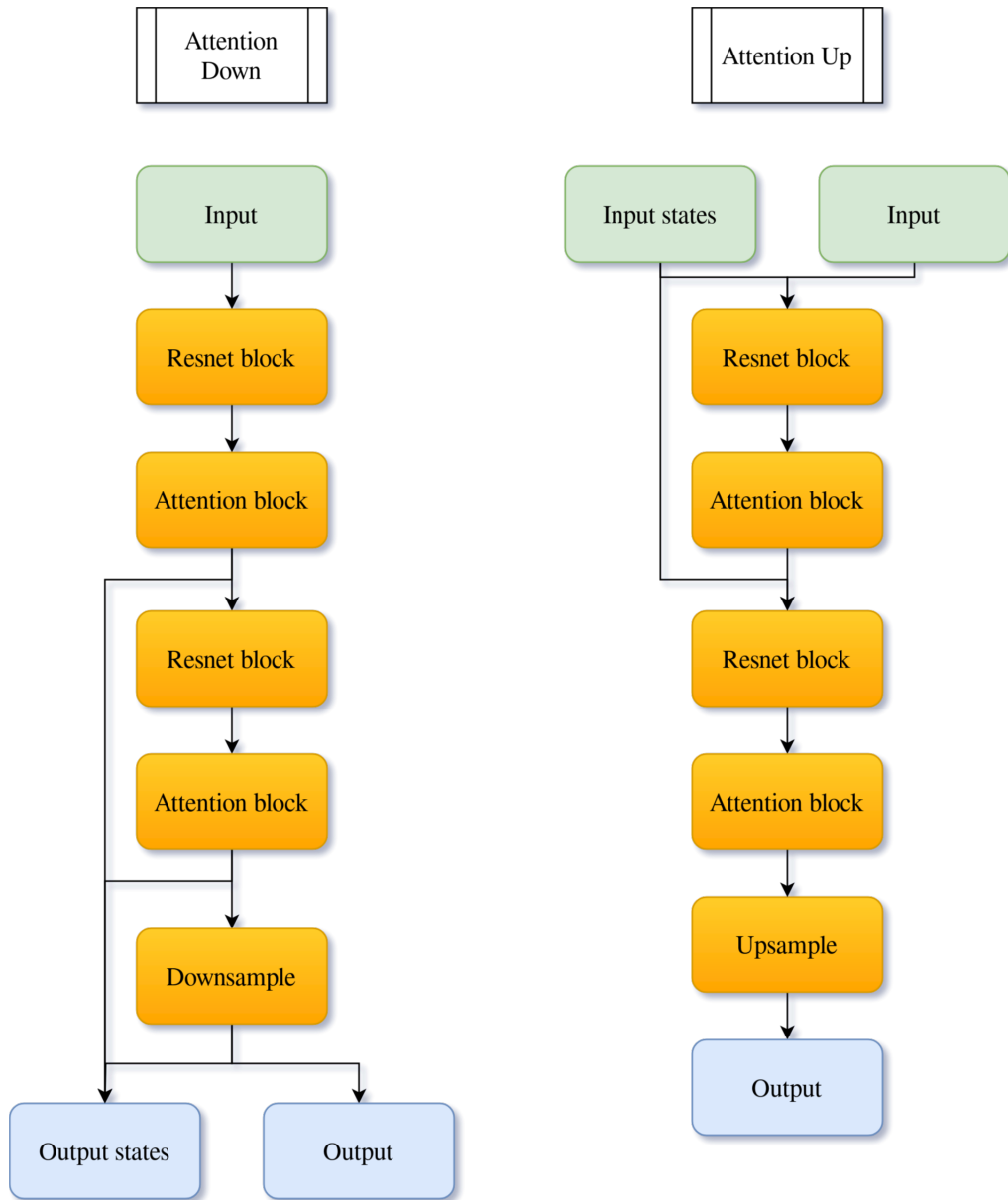


Figure 3.5: Attention downsample and upsample block architecture diagram

3.2.6 Mid block

Mid block is responsible for processing latent space. In this case latent space is not one dimensional so the resnet blocks with convolution are used, as well as attention blocks for learning the dependencies between individual parts of latent space.

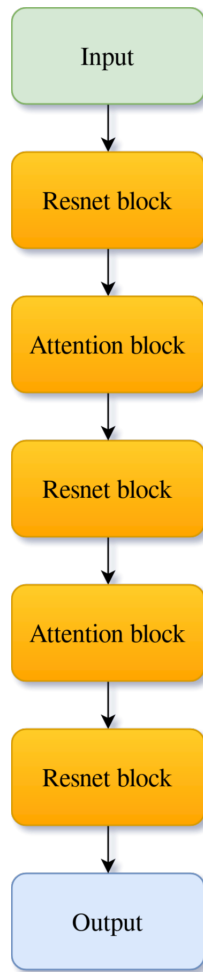


Figure 3.6: Mid block architecture diagram

3.2.7 Network architecture

U-Net model is an architecture used in image generation. It has an encoder to capture features, a bottleneck for extraction, and a decoder for image generation. The model has additional skip connections between encoder and decoder which help preserve fine details.

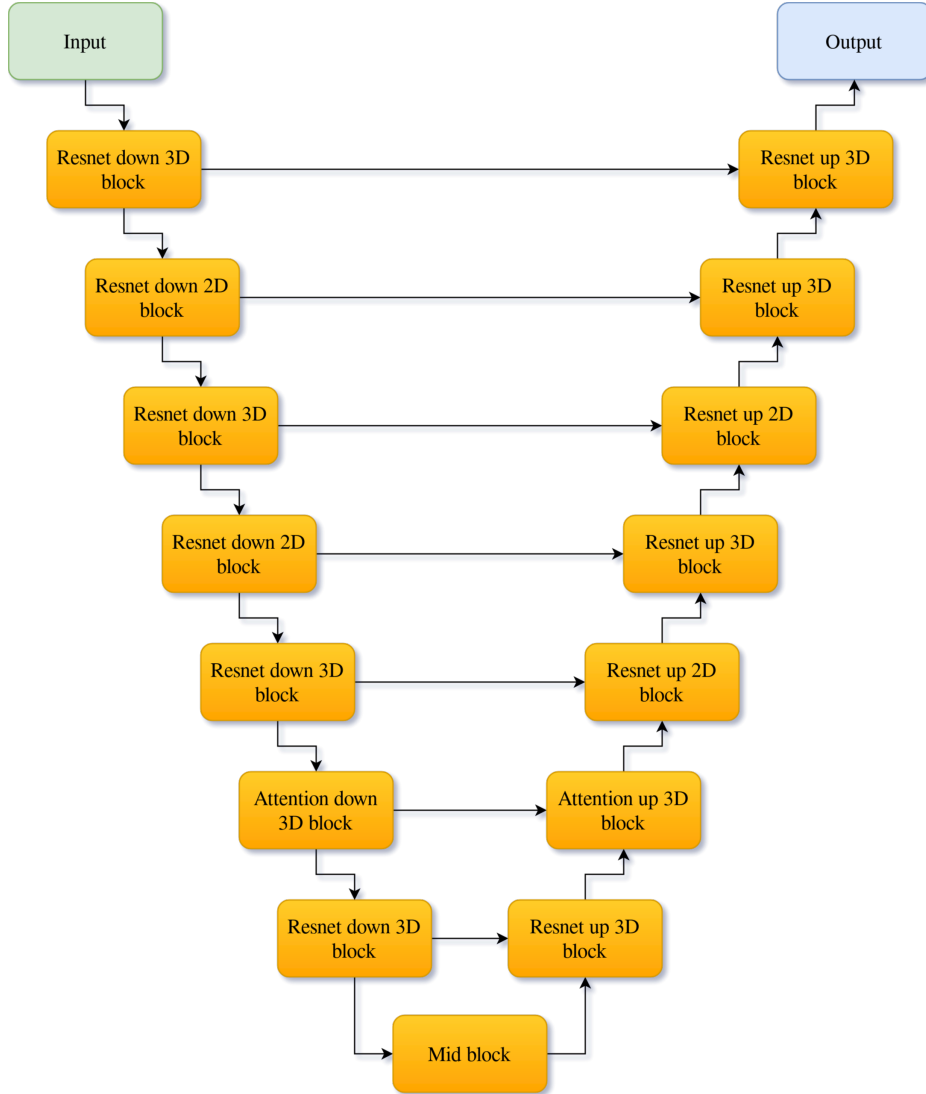


Figure 3.7: Network architecture

3.2.8 Training parameters

Batch size

In consideration of both the constraints posed by GPU memory limitations and the dataset's size, the decision was made to set the batch size to one.

Learning rate

A range of values, spanning from 10^{-7} to $3 \cdot 10^{-4}$, were systematically tested. It was observed that lower values within this range led to a slower learning pace and generated scans with considerably more noise. Conversely, as the values increased, the model's performance improved, with larger values yielding better results. However, it became evident that once the threshold of approximately $2 \cdot 10^{-4}$ was crossed, the model's stability during training became compromised, often becoming trapped in local minima.

In light of these findings, a careful evaluation led to the selection of the optimal value, which was determined to be 10^{-4} . This value struck a balance between achieving satisfactory results and maintaining training stability, making it the most suitable choice.

Number of epochs

The number of epochs was established at 2000 due to the observation that the model's loss reached a plateau at this juncture, and further training did not yield any substantial improvements in results.

3.2.9 Training script

In the source code the training script is provided in which, users can specify various training configurations at the start of the file. These configurations include selecting the training device, defining data dimensions, specifying the number of training epochs, setting the batch size, indicating the data directory, and more. After configuring these parameters, users can customize the neural network architecture by selecting building blocks.

The script then proceeds to partition the data, initiate the training process, and periodically save the model and generate samples at specified intervals during training epochs. Additionally, the script identifies and preserves the best-performing model based on its performance on a test dataset.

3.3 Dataset

The dataset contain a collection of 28 high-resolution computer tomography (CT) images that center on the prostate region. Each image has undergone meticulous hand-trimming to retain solely the pertinent anatomical features. This process results in a dataset that accentuates the vital elements essential for accurate interpretation.

These CT images grant a precise and detailed view of the prostate gland and its encompassing structures. The hand-trimming process has thoughtfully excluded irrelevant details and unrelated areas, leaving only a focused representation.

All scans in this dataset adhere to a standardized dimension of 512 pixels by 512 pixels, presented across 26 individual slices. This 3D arrangement permits a comprehensive examination of the prostate from various perspectives and depths. The uniform image size and multiplicity of slices contribute to a thorough analysis and a more precise understanding of the prostate's configuration and potential discrepancies.

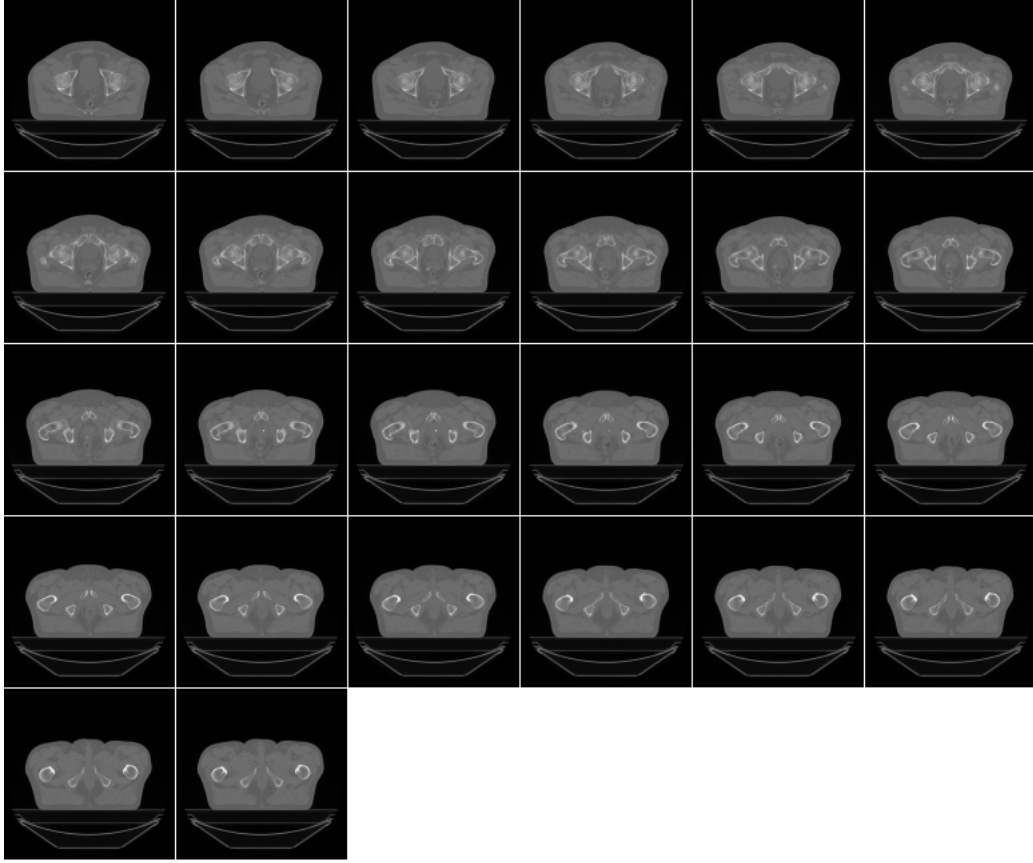


Figure 3.8: Example from dataset

The dataset underwent a random partitioning procedure, resulting in the creation of two distinct subsets: a training dataset and a validation dataset. This division was executed in an 80-20 ratio, leading to a training subset comprising 23 scans and a validation subset containing 5 scans.

Furthermore, to enhance the dataset's diversity and training potential, augmentation techniques were applied. Random zoom and flip operations were employed every epoch to augment the data. These augmentation methods introduce variations in scale and orientation, contributing to a more comprehensive and versatile dataset. The incorporation of such augmented data aids in training models that are better equipped to handle a wider range of real-world scenarios and variations.

Ultimately, all CT images were resized to 256 by 256 pixels, a necessary adjustment due to the limitations of GPU memory.

Chapter 4

Results

This chapter presents the results of performed studies involving generative neural networks tasked with generating realistic CT scans. The aim of this investigation was to evaluate the network's ability to produce accurate and visually coherent medical images.

4.1 Loss

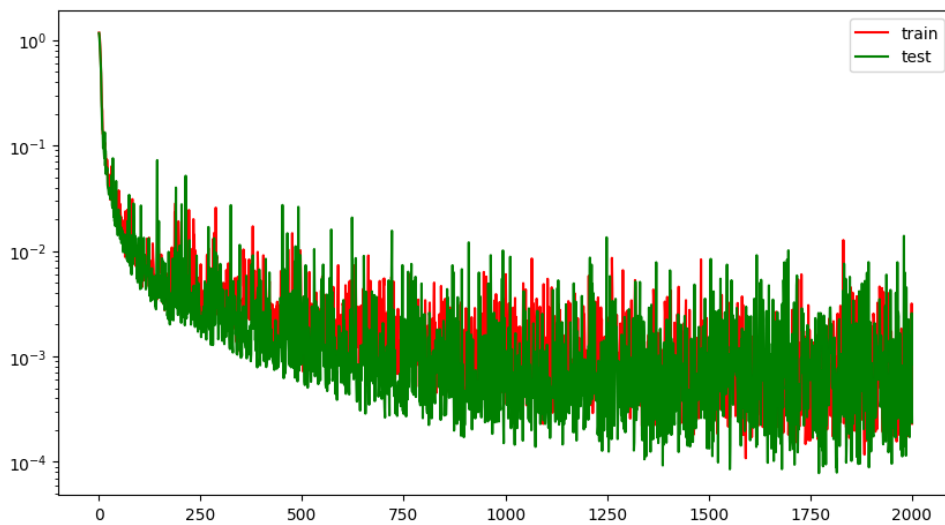


Figure 4.1: Loss history graph

Because of a relatively high learning rate, the graph shown above lacks clarity. To enhance its visibility, we calculate the average for every 10 epochs, resulting in a more visually accessible representation.

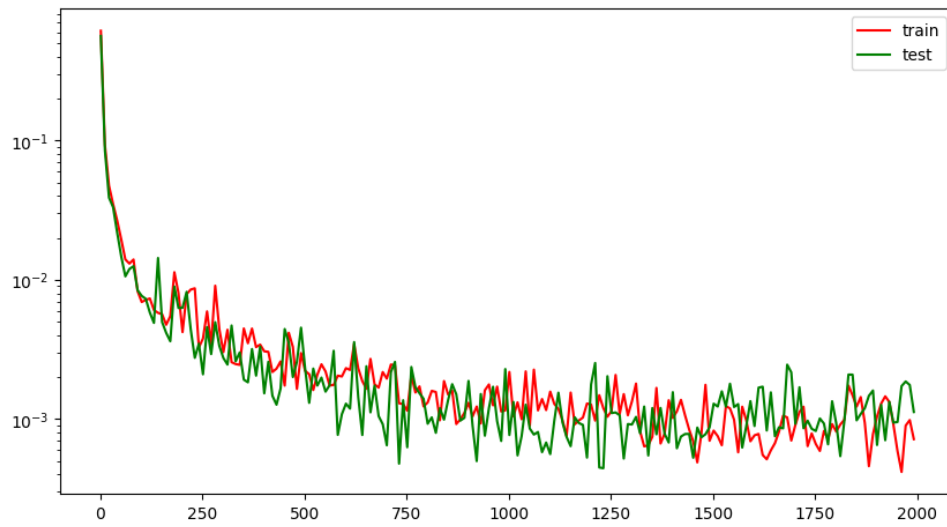


Figure 4.2: Average loss history graph

Both graphs utilize a logarithmic scale to display the training and test data loss. An observation drawn from these graphs suggests that the loss has reached a plateau, indicating that further training is unlikely to yield significant improvements in results.

4.2 Generated CT scans

4.2.1 Examples

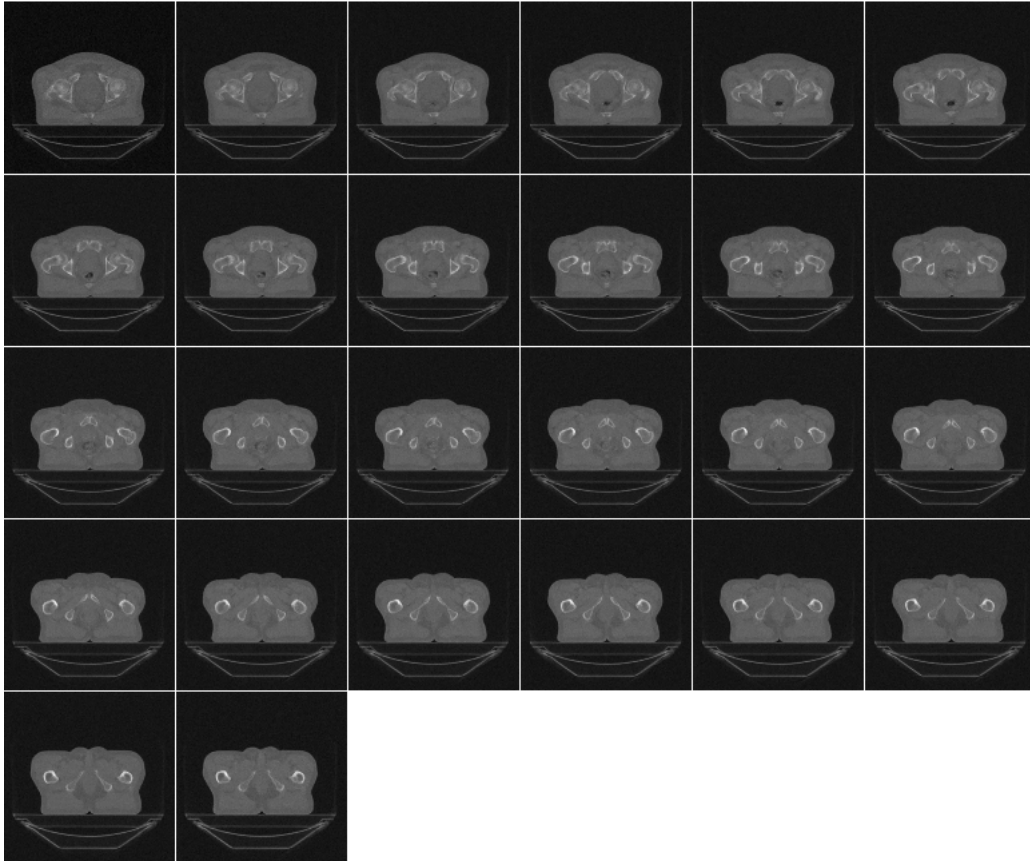


Figure 4.3: CT scan generated by the model

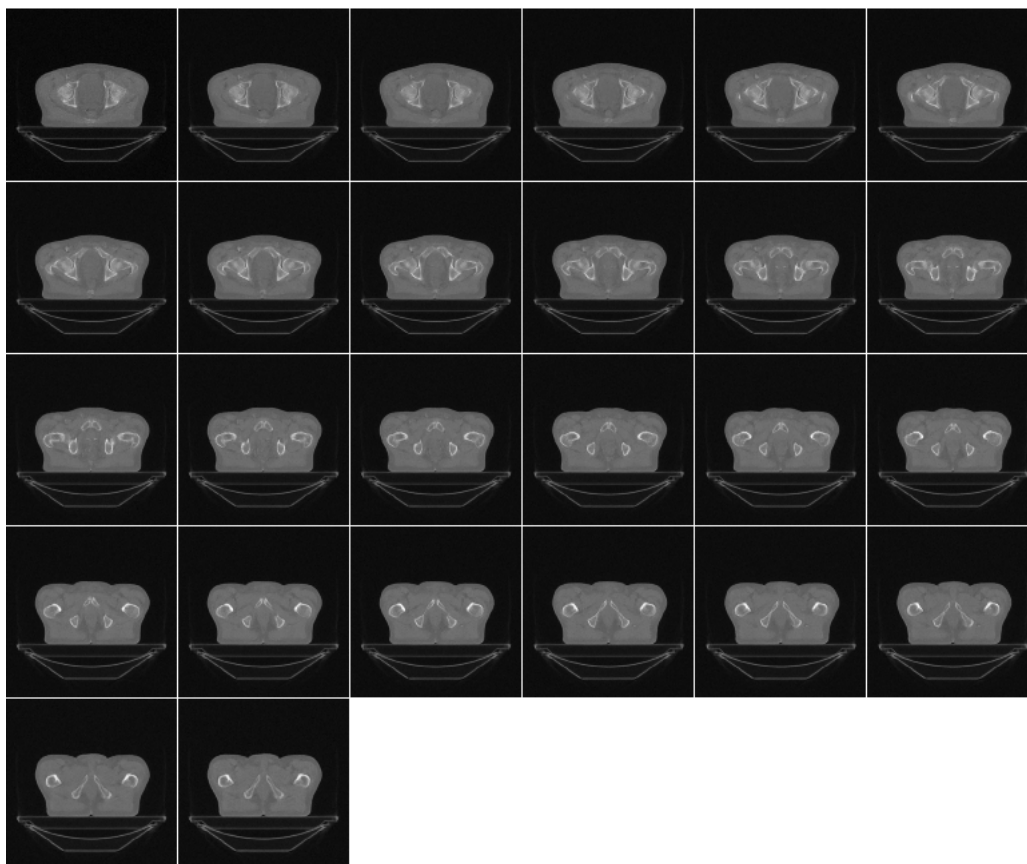


Figure 4.4: CT scan generated by the model

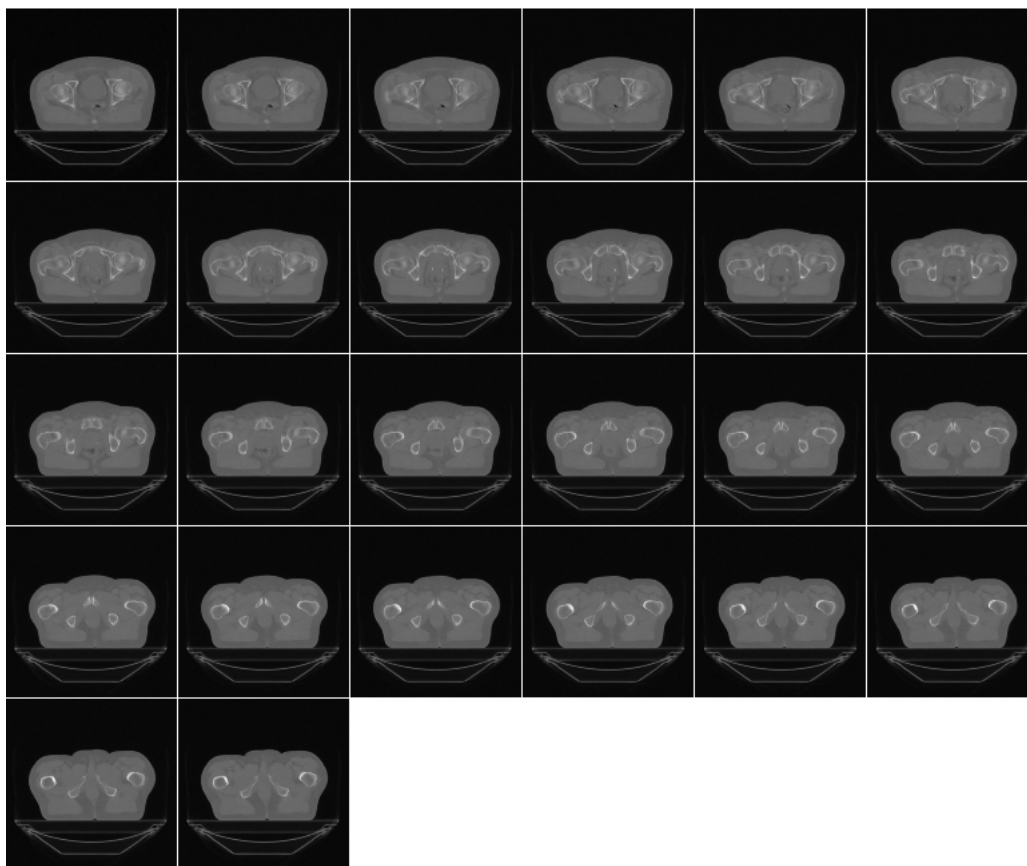


Figure 4.5: CT scan generated by the model

4.2.2 Visual Realism and Quality

Upon visual inspection, the generated CT scans exhibit a good level of realism and quality. Anatomical structures such as the prostate, bladder, and surrounding tissues are accurately portrayed, with textures and contrasts resembling those observed in actual CT scans. The model successfully captures the complex spatial relationships and proportions of anatomical structure.

4.2.3 Variability and Diversity

The network demonstrates proficiency in generating diverse images. It produces a spectrum of anatomical variations, encompassing different organ sizes, shapes, and orientations.

4.2.4 Comparison to original data

Comparing the generated CT images with their corresponding original counterparts reveals nuanced differences in various aspects. While the generated images bear a striking resemblance to the original CT scans in terms of anatomical structures and general features, there are certain distinctions worth noting. Notably, the generated CT images tend to exhibit slightly lower contrast levels in comparison to the originals, which could impact the visual clarity of certain structures. Additionally, a subtle increase in noise is observed in some of the generated images, which could potentially affect the interpretability of finer details. Furthermore, in some instances, the generated images may portray tissue textures that appear somewhat unnatural, suggesting room for improvement in capturing the intricate subtleties present in actual medical images.

4.3 Limitations

The current output of the model generates scans with a resolution of 256 by 256 pixels. However, it is important to note that this resolution is not enough to declare the generated samples have high quality. The limitation in resolution is primarily attributed to two key factors. First, there are constraints imposed by the available GPU memory, which dictates the practical upper limit for training process. Second, the underlying dataset itself has a resolution of 512 by 512 pixels. Consequently, the model is working within these constraints, resulting in the current resolution output.

Furthermore, it's worth emphasizing that evaluating the quality of these generated samples is a complex and require medical knowledge. The intricacies of medical imaging might only be evident to experts.

4.4 Future Directions

The next logical move would be to attempt generating higher-resolution samples by using multiple GPUs.

Future research endeavors could explore refining the network architecture for enhanced in image quality and anatomical accuracy. Expanding the study to larger datasets could further enrich the generative capabilities. Additionally, the model can be trained on datasets with different organs to check the performance in slightly different task.

Bibliography

- [1] <https://arxiv.org/pdf/2006.11239.pdf>
- [2] <https://arxiv.org/pdf/2102.09672.pdf>
- [3] <https://arxiv.org/pdf/2105.05233.pdf>
- [4] <https://arxiv.org/pdf/2112.10752.pdf>
- [5] <https://arxiv.org/pdf/2205.11487.pdf>
- [6] <https://lilianweng.github.io/posts/2021-07-11-diffusion-models/>
- [7] <http://jalammar.github.io/illustrated-stable-diffusion/>
- [8] <https://aman.ai/primers/ai/diffusion-models/>
- [9] <https://arxiv.org/pdf/2206.09453.pdf>
- [10] https://en.wikipedia.org/wiki/Diffusion_model
- [11] https://en.wikipedia.org/wiki/Kullback%E2%80%93Leibler_divergence
- [12] https://en.wikipedia.org/wiki/Variational_autoencoder
- [13] <https://arxiv.org/pdf/1505.04597v1.pdf>
- [14] <https://en.wikipedia.org/wiki/U-Net>
- [15] <https://github.com/CompVis/stable-diffusion>
- [16] <https://ommer-lab.com/research/latent-diffusion-models/>
- [17] Ian Goodfellow and Yoshua Bengio and Aaron Courville, Deep Learning, 2015
<https://www.deeplearningbook.org/>
- [18] <https://huggingface.co/blog/annotated-diffusion>
- [19] <https://arxiv.org/pdf/1706.03762.pdf>
- [20] [https://en.wikipedia.org/wiki/Attention_\(machine_learning\)](https://en.wikipedia.org/wiki/Attention_(machine_learning))
- [21] <https://w.wiki/7MW8>
- [22] <https://machinelearningmastery.com/the-attention-mechanism-from-scratch/>

- [23] Analysis of the quality of CT medical data generation using a pre-trained GAN model, Michał Orlewski, 2023
- [24] <https://www.python.org/>
- [25] <https://pytorch.org/>
- [26] <https://monai.io/>
- [27] <https://huggingface.co/docs/diffusers/index>
- [28] <https://github.com/huggingface/diffusers>
- [29] https://en.wikipedia.org/wiki/Residual_neural_network
- [30] <https://pytorch.org/docs/stable/index.html>